ACS OMEGA

http://pubs.acs.org/journal/acsodf

Article

Hydrogen–Deuterium Addition and Exchange in *N*-Ethylmaleimide Reaction with Glutathione Detected by NMR Spectroscopy

G. A. Nagana Gowda,* Vadim Pascua, Fausto Carnevale Neto, and Daniel Raftery*

Cite This: *ACS Omega* 2022, 7, 26928–26935

Read Online

ACCESS | Metrics & More | Article Recommendations | Supporting Information

ABSTRACT: Glutathione (GSH) is an important and ubiquitous thiol compound abundantly present in virtually every living cell. It is a powerful antioxidant critically required to protect cells from oxidative damage and free radical injury. Its quantification in *ex vivo* analysis remains a major challenge because it spontaneously oxidizes to form glutathione disulfide. *N*-Ethylmaleimide (NEM) is a well-known Michael acceptor, which reacts rapidly and irreversibly with thiol and prevents disulfide bond formation. Based on thiol conjugation to NEM, recently, the concentration of GSH was determined in human blood using NMR spectroscopy [*Anal. Chem*, 2021, 93(44): 14844−14850]. It was found that hydrogen−deuterium addition and exchange occur during the thiol−maleimide reaction as well as NMR analysis, generating a series of poorly explored diastereomers/isotopomers. Here, we establish a general NMR approach to identify the thiosuccinimide diastereomers/isotopomers derived from the thiol−maleimide reaction. The thiol-Michael addition reaction was conducted for GSH and another thiol compound, cysteine, separately, using D_2O and H_2O. The conjugates were characterized by $^1H/^{13}C$ 1D/2D NMR under different solvent, buffer, and pH conditions. The Michael addition combined with the H/D exchange formed twelve unique diastereomers/isotopomers. NMR measurements allowed the distinct assignment of all structures in solutions and quantification of H/D addition and exchange. Interestingly, the deuterium exchange rate was dependent on structure, pH, and buffer. The elucidation of the thiol−maleimide reaction and H/D exchange mechanism can potentially impact areas including metabolomics, small molecule synthesis, and bioconjugation chemistry.

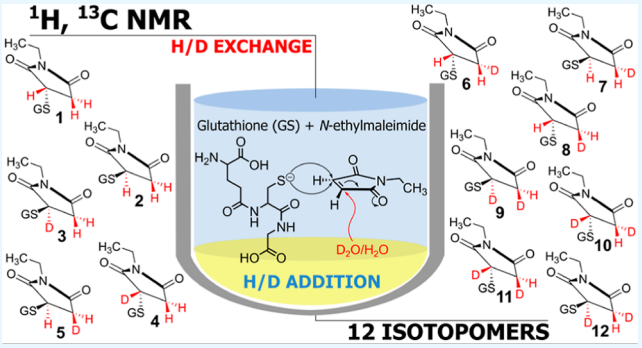

INTRODUCTION

Maleimides are Michael acceptors that are known to react with thiols in the pH range of 6.5−7.5.[1−3] In general, maleimides are more reactive than other Michael acceptors[4] and represent an important class of substrates for chemical and biological applications. The maleimide ring strain imposed by the alkene moiety enhances the electrophilic nature of the conjugated imide functionality.[5] Furthermore, the nature of the solvent, basic environment, and the type of thiol play important roles in the reaction kinetics and selectivity in thiol−maleimide reactions. Owing to its simplicity, efficiency, and wide utility, the thiol−maleimide reaction is characterized as a click chemistry reaction.[2,6] Hence, the reaction has implications in numerous areas including small molecule synthesis, bioconjugation chemistry, and multifunctional materials.[3]

N-Ethylmaleimide (NEM) is known to react with thiols rapidly and irreversibly. Since the first report more than 70 years ago,[7] the quantitative reaction of NEM with thiol compounds has been widely used to assay thiol-group-containing compounds including proteins, peptides, and small molecules in biological mixtures.[8−13] Glutathione (reduced form, GSH) is a highly abundant non-protein thiol in live cells. It is an important and ubiquitous cellular antioxidant critically required to protect cells from oxidative damage and free radical injury. As with other thiols, it is practically impossible to analyze GSH in its native form in biological samples because the active form (GSH) spontaneously gets converted to the oxidized form glutathione disulfide (GSSG). To block GSH oxidation, NEM is widely used such that the reacted GSH can then be analyzed using a variety of analytical techniques including spectrophotometry,[14,15] fluorometry,[16−18] and mass spectrometry.[19−24] The chemical reaction of NEM and GSH is instantaneous and it does not need any catalyst for the reaction. In addition, the product formed is stable for long periods, at least several months.[25] These characteristics offer experimental simplicity and are attractive for applications including the quantitation of thiol compounds.

Received: June 3, 2022
Accepted: July 4, 2022
Published: July 18, 2022

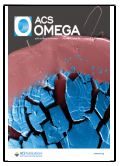

© 2022 The Authors. Published by American Chemical Society

https://doi.org/10.1021/acsomega.2c03482
ACS Omega 2022, 7, 26928−26935

Recently, we demonstrated the utility of the NEM reaction with GSH for the quantitative analysis of GSH in biological samples in human whole blood using *ex vivo* nuclear magnetic resonance (NMR) spectroscopy.[26] The new NMR method enables quantitation of the very unstable GSH as well as other labile metabolites including the major redox coenzymes (NAD^+, NADH, $NADP^+$, and NADPH) and energy coenzymes (ATP, ADP, and AMP) in biological mixtures, all in one step. Furthermore, interestingly, it was found that hydrogen−deuterium addition and exchange occur during the thiol NEM reaction and NMR analysis, generating a series of diastereomers/isotopomers. While the thiol-Michael addition reaction has been known for a very long time, and the formation of two diastereomers from the reaction is well known,[25,27,28] the generation of diastereomers/isotopomers has not been well explored to date. In this study, we establish a general NMR approach to correctly identify the thiosuccinimide diastereomers/isotopomers derived from the thiol NEM reaction as depicted in Figure 1. The thiol-Michael addition

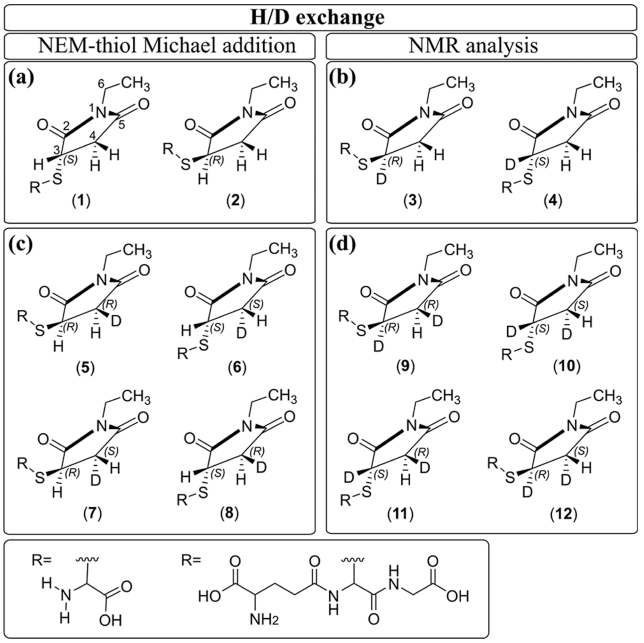

Figure 1. Diastereomers/isotopomers formed by the Michael addition reaction in (a) H_2O and (c) D_2O solvents, and by H/D exchange during NMR analysis (b,d). R in the structures refers to GSH or Cys. For each diastereomer/isotopomer, the configuration for the chiral carbon centers is indicated by *R* or *S*.

was conducted for GSH and cysteine (Cys), separately, using D_2O and H_2O. The conjugates were characterized by $^1H/^{13}C$ one-dimensional (1D)/two-dimensional (2D) NMR under different solvent, buffer, and pH conditions. These findings have implications in numerous areas including metabolomics, small molecule synthesis, isotopic enrichment, and bioconjugation chemistry.

MATERIALS AND METHODS

Chemicals and Solvents. Monosodium phosphate (NaH_2PO_4), disodium phosphate (Na_2HPO_4), ammonium bicarbonate (NH_4HCO_3), trimethylsilyl propionic acid-d_4 sodium salt (TSP), acetanilide, *N*-ethylmaleimide (NEM), GSH (reduced, GSH), Cys, hydrochloric acid, and sodium hydroxide were obtained from Sigma-Aldrich (St. Louis, MO) or Fisher (Waltham, MA). Deuterium oxide (D_2O) was procured from Cambridge Isotope Laboratory (Tewksbury, MA). Deionized (DI) water was purified using an in-house Synergy Ultrapure Water System from Millipore (Billerica, MA). All chemicals and solvents were used without further purification.

Stock Solutions of GSH, Cys, and NEM. GSH (50 mM), Cys (50 mM), and NEM (120 mM) solutions were prepared using DI water and D_2O by weighing appropriate amounts.

Buffer Solutions with Internal Standards. Phosphate buffer solution (100 mM, pH = 7.4) was prepared by dissolving 1124.0 mg of anhydrous Na_2HPO_4 and 249.9 mg of anhydrous NaH_2PO_4 in 100 g D_2O or DI water. Ammonium bicarbonate buffer solution (50 mM, pH = 8.4) was prepared by dissolving 400 mg of ammonium bicarbonate in 100 g D_2O. TSP (100 μM) was added to the above solutions to serve as a chemical shift reference.

NEM Reaction with the Thiols. GSH (40 μL, 50 mM) stock solution in H_2O or D_2O solvent was treated with six-fold excess of (NEM) (100 μL, 120 mM) solution in H_2O or D_2O, respectively. The solutions were mixed using a vortexer for 30 s to derivatize GSH with NEM. Then, the H_2O/D_2O solvents, along with the excess (unreacted) NEM, were removed by drying the solutions using a stream of nitrogen gas, as described in a recent study, where NEM was conjugated with blood GSH.[26] The dried samples were dissolved in 600 μL D_2O and the pH was adjusted as needed to 6.0, 7.0, or 8.0 using hydrochloric acid or sodium hydroxide. Separately, the dried samples were dissolved in 600 μL phosphate buffer prepared in H_2O or D_2O (100 mM, pH = 7.5) or ammonium bicarbonate buffer prepared in D_2O (50 mM, pD = 7.8). The solutions were transferred to 5 mm NMR tubes for analysis. Similarly, the NEM reaction with Cys was conducted and samples were prepared for NMR analysis. Four to ten replicates were used for each condition of the hydrogen−deuterium addition and exchange reactions.

NMR Spectroscopy. NMR experiments were performed at 298 K on a Bruker AVANCE III 800 MHz spectrometer equipped with a cryogenically cooled probe and *z*-gradients suitable for inverse detection. The NOESY pulse sequence with residual water suppression using presaturation with or without combining with pulsed-field gradients was used for ^1H 1D NMR experiments. The spectral width of 9615 or 10,204 Hz; 3 or 55 s recycle delay; 32, 64, or 128 transients; and 32 or 64 K time-domain points were used for ^1H 1D NMR experiments. The free induction decay (FID) signals were Fourier transformed after zero filling by a factor of two and multiplied using an exponential window function with a line broadening of 0.3 Hz.

Separately, for the GSH−NEM compounds obtained from the reactions in H_2O as well as D_2O, 1D ^{13}C, and 2D NMR experiments were performed using H_2O/D_2O (90:10 v/v), D_2O, or D_2O buffer solvents. 1D ^{13}C spectra were obtained using the "zgpg" pulse sequence and a spectral width of 40760 Hz, 2 s recycle delay, 1000 transients, and 128 K time-domain points. The FID signals were Fourier transformed after zero filling by a factor of two and multiplied using an exponential window function with a line broadening of 3.0 Hz. The 2D NMR experiments performed included $^1H-^1H$ COSY (correlated spectroscopy), $^1H-^{13}C$ heteronuclear single quantum coherence (HSQC), and $^1H-^{13}C$ heteronuclear multiple bond correlation (HMBC). Spectra were obtained in magnitude mode for COSY and HMBC, and phase-sensitive

https://doi.org/10.1021/acsomega.2c03482
ACS Omega 2022, 7, 26928−26935

mode using echo-*anti*-echo mode for HSQC experiments. COSY experiments were performed using the "cosygpprqf" pulse sequence and a spectral width of 10,204 Hz in both dimensions. FID signals were obtained for 512 t_1 increments, each with 2048 complex data points. The number of transients was 4 and the relaxation delay was 2.0 s. The obtained 2D data were zero-filled to 4096 and 1024 points in the t_2 and t_1 dimensions, respectively. Gaussian and unshifted sine-bell window functions were applied to the t_2 and t_1 dimensions, respectively, before Fourier transformation. HSQC and HMBC experiments were performed using the "hsqcetgpsisp2.2" and "hmbcgplpndprdf" pulse sequences, respectively. Spectral widths of 8802 Hz (^{1}H) and 30,186 Hz (^{13}C) for HSQC and 8620 Hz (^{1}H) and 40,760 Hz (^{13}C) for HMBC were used. FID signals were obtained with 256 or 512 t_1 increments, each with 2048 and 4096 complex data points for HSQC and HMBC, respectively. The number of transients used was 8 or 16 and the relaxation delay was 1.05 s. The obtained 2D data were zero-filled to 4096 and 1024 points in t_2 and t_1 dimensions, respectively. A 45° shifted squared sine-bell window function was applied to both dimensions before Fourier transformation. The chemical shift scales were calibrated based on the TSP signal for ^{1}H and ^{13}C.

Spectral Assignment and Quantitation of Diastereomers/Isotopomers. Assignment of peaks from the products of the NEM reaction with GSH and Cys were based on the results of our recent study,[26] the comparison with NMR spectra of the reactants, and the comprehensive analyses of 1D and 2D NMR spectra of NEM reacted compounds. Quantitation of the diastereomers/isotopomers formed by H/D addition and/or exchange reactions were made based on the peak areas of methine (CH) and methylene (CH_2) hydrogens of the thiosuccinimide ring under different solvent, buffer, and pH conditions. Bruker software, TopSpin version 3.6.1 or 4.1.0, was used for NMR data acquisition, processing, and analyses.

RESULTS AND DISCUSSION

The Michael addition reaction occurred as soon as the stock solution of GSH or Cys was mixed with NEM. The formation of thiol−NEM conjugates was rapid and irreversible, promoted by thiolate ion generation in the highly polar solvent.[2] At pH ∼7, the 1,4 nucleophilic thiol addition to the C=C bond in maleimide takes place on both sides of the two sp^2 carbons; only two spatial configurations are possible for the new sulfite bond because both α,β-unsaturated carbonyls are similar due to the C_2 axis of symmetry. The bulkier *N*-substituted maleimide potentially modulates the regioselectivity of the reaction. The thiolate-Michael reaction was associated with hydrogen/deuterium addition at C4, a consequence of ketonization of the enolate and the solvent used (Figures 2 and S1a).

We investigated the products of the maleimide reaction in H_2O or D_2O using ^{1}H and ^{13}C 1D and 2D NMR under different solvent, buffer, and pH conditions. We first examined samples in acidic conditions using H_2O at pH = 3.2 or D_2O at pD = 3.3. Two diastereomers (**1** and **2**) were formed during the thiol−maleimide reaction in H_2O (Figure 1a). Figures 3a and S2a show ^{1}H NMR spectra for **1** and **2**. The two structures show methine (C3) hydrogen peaks at ∼4.06 ppm and methylene (C4) hydrogen peaks at ∼2.69 and 3.29 ppm, with slightly different chemical shifts for the two (red and blue peaks in Figure 3a). The thiol-Michael addition in D_2O, on the other hand, generated four diastereomers/isotopomers (**5**−**8**, Figure 1c). The ^{1}H NMR spectrum showed four sets of convoluted peaks for methine and methylene hydrogens, at C3 and C4, respectively, because of partially overlapped peaks (Figures 3c and S2c; peaks are shown in four different colors in Figure 3c). Interestingly, the methylene hydrogen peaks exhibited two different intensities with a ratio ∼65:35; peak intensities for hydrogens *cis* to methine hydrogens (**5**, **6**, see brown and yellow in Figure 1c) were higher than those that are trans to methine hydrogens (**7**, **8**, see green and blue peaks in Figure 3c). This difference in the yields can be explained by the regioselective ketonization of the enolate, which favors deuteration at C4 on the opposite side of the sulfide bond because of the steric hindrance of the S-atom (Figure 2).

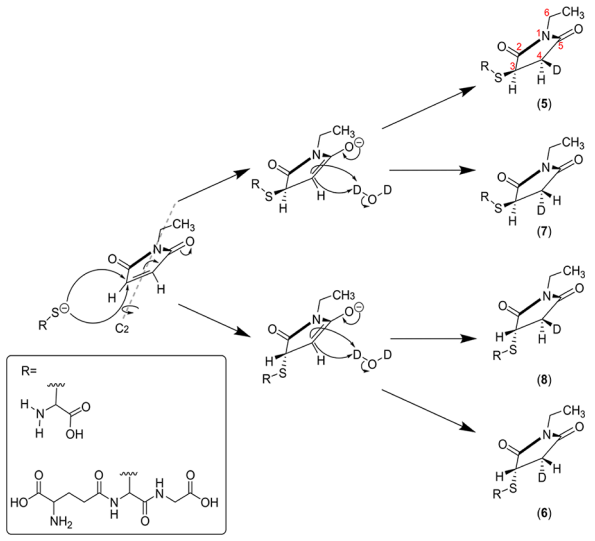

Figure 2. Michael addition reaction in D_2O solvent (see Figure S1a for the reaction in H_2O). R in the structures refers to GSH or cysteine.

When the samples were reconstituted in phosphate buffer/D_2O at pD = 7.5, ammonium bicarbonate buffer/D_2O at pD = 8.4, or D_2O at pD = 6.0, 7.0, or 8.0 we found slow (Figure S3), and reversible (Figure S4) H/D exchange at C3. For the structures **1** and **2**, the exchange generated two chiral (H/D) isotopomers, **3** and **4** (Figures 1b and S1b), characterized by two sets of doublets at ∼2.7 and 3.28 ppm due to $^2J_{HH}$ coupling between the two methylene hydrogens (Figures 3b and S2b). For structures **5**−**8**, the H/D exchange led to four isotopomers, **9** to **12** (Figure 1d), and Figures 3d and S2d show peaks for all four structures. Overall, the Michael addition and H/D exchange resulted in 12 distinct isotopomers (Figure 1) and all 12 were distinctly identified by NMR (Figures 3 and S2).

For further validation of the isotopomer formation and identification, the structures were investigated using 2D NMR. Figure 4 shows portions of typical 2D ^{1}H−^{1}H COSY spectra. The 2D NMR peaks from the methine and methylene hydrogens from the thiosuccinimide ring are connected by red dashed lines, vertically and horizontally. Figure 4a,b show spectra for the reaction in H_2O. The spectrum in Figure 4a was obtained in D_2O (pD = 3.3) and the spectrum shown in Figure 4b was obtained in phosphate buffer/D_2O (pD = 7.5). Figure 4a represents structures **1** and **2** and shows peaks for the thiosuccinimide methine (at C3) and methylene (at C4) hydrogens as seen from the 2D NMR cross-peaks among all

https://doi.org/10.1021/acsomega.2c03482
ACS Omega 2022, 7, 26928−26935

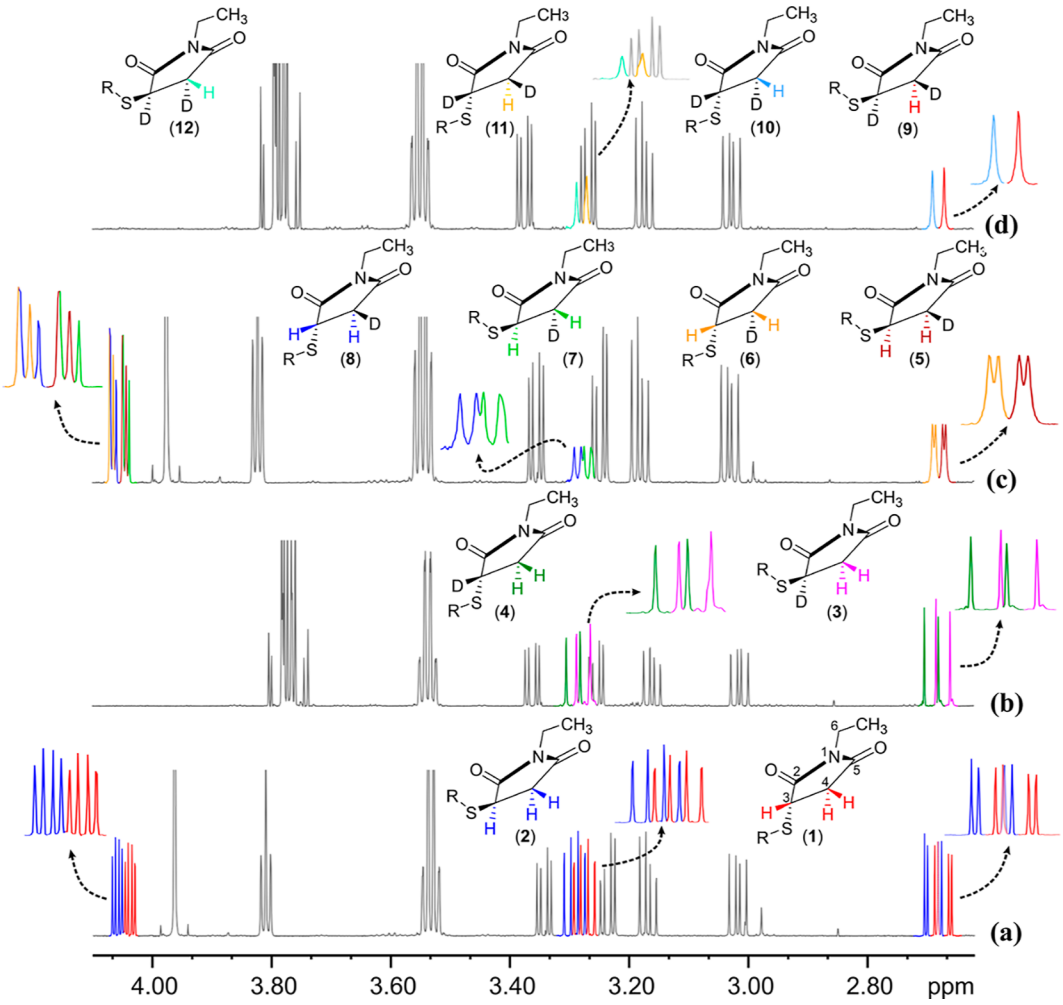

Figure 3. Portions of ^{1}H NMR spectra highlighting the characteristic peaks for 12 diastereomers/isotopomers formed by the Michael addition reaction of GSH with NEM and H/D exchange. In each spectrum, methine or methylene hydrogen peaks for each isotopomer are shown by the same color. Spectra (a,b) are for the reaction in H_2O: (a) spectrum obtained in D_2O solvent (pD = 3.3) corresponding to structures **1** and **2**; (b) spectrum obtained in phosphate buffer/D_2O (pD = 7.5) corresponding to structures **3** and **4**; (c,d) are for the reaction in D_2O: (c) spectrum obtained in D_2O solvent (pD = 3.3) corresponding to structures **5** to **8**; (b) spectrum obtained in phosphate buffer/D_2O (pD = 7.5) corresponding to structures **9 to 12** (see also Figure S2).

three hydrogens. The two methylene hydrogens show peaks at different chemical shifts (~2.7 and 3.3 ppm). Figure 4b represents structures **3** and **4**. Here, the 2D NMR cross-peaks are observed only between the two methylene hydrogens because the methine hydrogen is absent due to the exchange with D. Similarly, Figure 4c,d show spectra for the GSH−NEM reaction in D_2O. The spectrum in Figure 4c was obtained in D_2O (pD = 3.3) and the spectrum shown in Figure 4d was obtained in phosphate buffer/D_2O (pD = 7.5). Figure 4c represents the structures **5**−**8**; and Figure 4d represents the structures **9**−**12**. The 2D NMR cross-peaks between the two methylene hydrogens are absent in Figure 4c because one of the hydrogens is replaced by D during the Michael addition reaction in D_2O. In Figure 4d, none of the 2D NMR cross-peaks is seen because the methine hydrogen exchanges with D from D_2O solvent and one of the methylene hydrogens is replaced by D during the Michael addition in D_2O. As further evidenced for H/D addition and exchange, Figures S5−S8 show overlays of ^{1}H−^{13}C 2D HSQC (blue cross-peaks) and ^{1}H−^{13}C 2D HMBC (red cross-peaks) spectra. A few characteristic 2D NMR peaks that establish the reaction of GSH with NEM and H/D addition and exchange are enclosed within rectangular boxes. The H/D addition and exchange are indicated by the absence or broadening of ^{1}H/^{13}C peaks for the methine (at C3) and methylene (at C4) hydrogens/carbons. For example, in Figure S5 ^{1}H/^{13}C 1D/2D NMR peaks for both C3 methine and C4 methylene groups are observed as anticipated for structures **1** and **2**. In Figure S6, peaks are missing for the methine hydrogen and the C3 carbon peak is invisibly broad due to H/D exchange (structures **3** and **4**); however, 2D peaks due to the long-range hydrogen/carbon couplings are still clearly seen. In Figure S7, the C4 carbon 1D NMR peak is broad due to the attached deuterium (structures **5**−**8**), whereas in Figure S8, in accordance with the structures, **9**−**12**, peaks for the methine hydrogens are missing and peaks for C3 and C4 carbons are broad due to deuterium exchange/addition. As anticipated, a correlation between ^{1}H and ^{13}C chemical shifts could be seen in all 2D NMR spectra (Figures S5−S8).

The NMR peak areas of the thiosuccinimide methine and methylene hydrogens (at C3 and C4) changed dramatically due to H/D exchange (Figure 5 and Tables S1 and S2). At higher pH/D, the keto−enol equilibrium caused the acidic α-

https://doi.org/10.1021/acsomega.2c03482
ACS Omega 2022, 7, 26928−26935

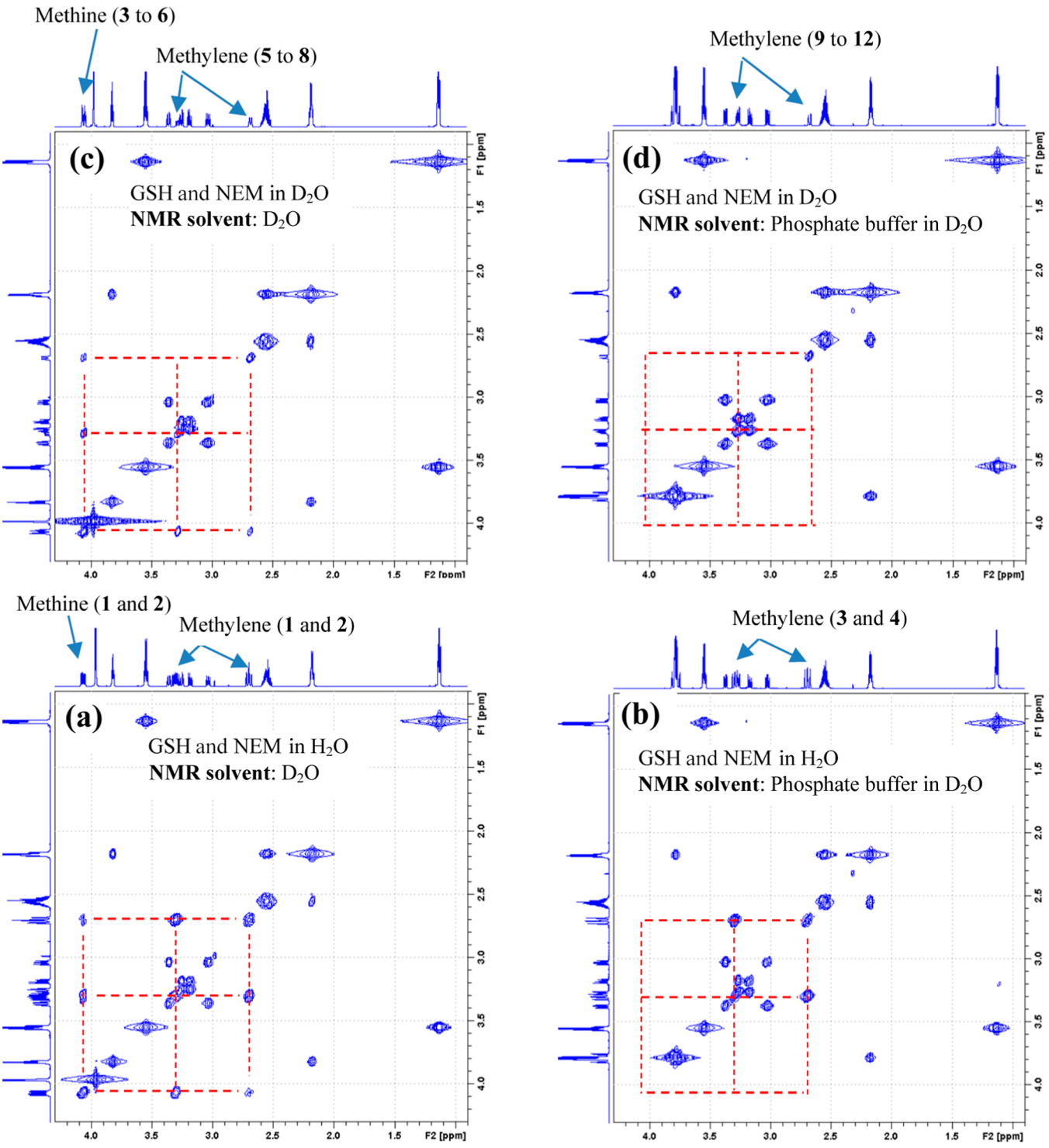

Figure 4. Portions of 2D $^{1}H-^{1}H$ COSY NMR spectra of mixtures from the reaction of GSH with NEM. For (a,b), the reaction was in H_2O solvent; spectra were obtained in D_2O (pD = 3.3) for (a) and phosphate buffer (100 mM, pD = 7.5) in D_2O for (b); for (c,d), the reaction was in D_2O; spectra were obtained in D_2O (pD = 3.3) for (c) and phosphate buffer (100 mM, pD = 7.5) in D_2O for (d). The characteristic thiosuccinimide methine and methylene peaks are highlighted. (a) corresponds to structures **1** and **2**; (b) corresponds to structures **3** and **4**; (c) corresponds to structures **5** to **8**; and (d) corresponds to structures **9** to **12**. Note, in (a), both methine and methylene H atoms are observed as seen by the 2D NMR cross-peaks among all the three Hs (connected by red dashed lines); in (b), 2D NMR cross-peaks are observed only between the two methylene Hs because the methine H is exchanged with D; in (c), 2D NMR cross-peak between the two methylene H is absent because one of the H atoms is substituted by D; and in (d), none of the 2D NMR cross-peaks is seen because one of the methylene H atoms is substituted by D and the methine H is exchanged with D.

hydrogen at C3 to exchange with deuterium. The peak area of methine hydrogens decreased with increasing pH/D, reaching ~15% or lower at pH = 8.0 (Figure 5a,c). Unlike the Michael addition, where the S-atom determines the stereochemistry of the enolate ketonization, the H/D exchange proceeds with a transition state where the C3 carbon is sp^2 hybridized.

https://doi.org/10.1021/acsomega.2c03482
ACS Omega 2022, 7, 26928−26935

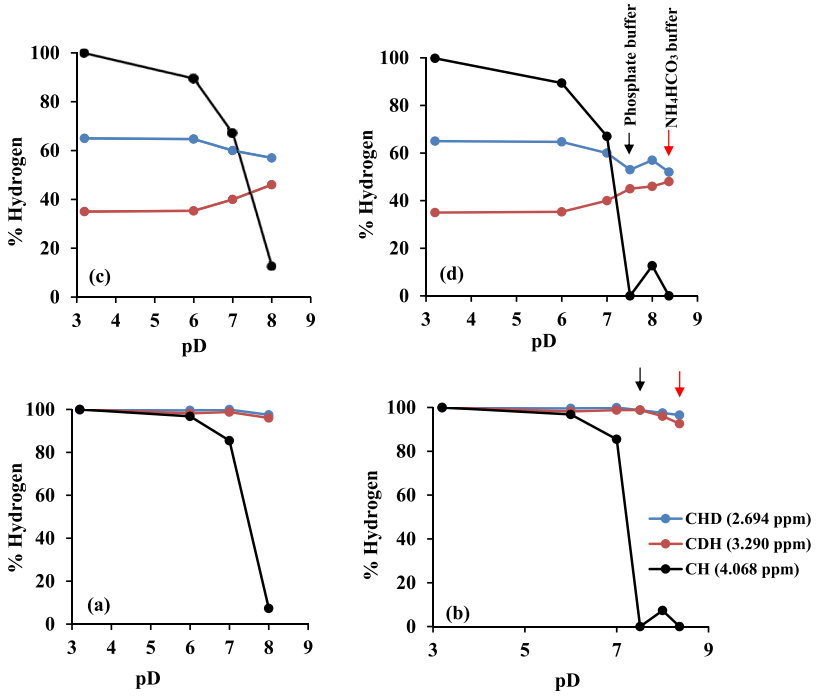

Figure 5. Percentage of methine and methylene Hs left after H/D addition and exchange for the NEM−GSH reaction. The reaction was performed in H_2O for (a,b), and in D_2O for (c,d). The black and red arrows in (b,d) indicate that the samples were in phosphate buffer or ammonium bicarbonate buffer.

Interestingly, the ratio between the two methylene hydrogens changed from 65:35 at pH/D 3.3, to 55:45 at pH/D > 8.0 (Figure 5c). The results indicated that the methylene H/D isotopomers gradually approach the ratio 1:1 because of the H/D exchange arising from isomerization of the diastereomers.[27] Phosphate and ammonium bicarbonate buffers caused higher H/D exchange when compared to D_2O or H_2O alone (Figure 5b,d). For example, while the methine hydrogen was fully exchanged with D in phosphate buffer (pH = 7.5), the exchange was in the range of 85−90% in D_2O solvent even at pH = 8.0. These results indicate that the anions of the buffers exhibit additional effects on the H/D exchange at both C3 and C4. The keto−enol tautomerism can be accelerated by both acidic and alkaline environments; however, our data support the previous observation that the base-catalyzed mechanism favors the H/D exchange, whereas the formation of an enolate intermediate was preferred over acid-catalyzed ketonization due to the sulfide bond.[29]

The reaction between Cys and NEM also formed two diastereomers with similar H/D addition and exchange mechanisms (Figure S9). In phosphate buffer, however, the ratio between the two diastereomers changed from ∼50:50 in D_2O to ∼41:59, unlike the reaction with GSH (Figure S10). Such a difference in the ratio between the diastereomers for Cys has not previously been reported to the best of our knowledge.

Taken together, the data show how the thiol NEM reaction generates a series of isotopomers under different solvent/buffer/pH conditions. Understanding how various isomers are formed and interpreting their NMR spectra are important steps to translating molecular information into biological knowledge. The identification of these isotopomers potentially has implications in areas such as metabolomics, small molecule synthesis, and bioconjugation chemistry. In the metabolomics field, for instance, the simple click chemistry reaction offers a simple route to generate deuterium-labeled internal standards for absolute quantitation of the highly unstable thiol compounds.

■ ASSOCIATED CONTENT

Supporting Information

The Supporting Information is available free of charge at https://pubs.acs.org/doi/10.1021/acsomega.2c03482.

Michael addition reaction in H_2O and H/D exchange mechanism, NMR spectra of the GSH−NEM reaction highlighting peaks for various isomers, time dependence of products of the GSH−NEM reaction in D_2O buffer, NMR spectra that show reversible H−D exchange in the reacted NEM ring, HSQC and HMBC spectra in D_2O of GSH−NEM products synthesized in H_2O, HSQC and HMBC spectra in D_2O buffer of GSH−NEM products synthesized in H_2O, HSQC and HMBC spectra in D_2O of GSH−NEM products synthesized in D_2O, HSQC and HMBC spectra in D_2O buffer of GSH−NEM products synthesized in D_2O, spectra in D_2O/D_2O buffer of Cys−NEM products synthesized in H_2O/D_2O, spectra highlighting the altered ratio between the two diastereomers for Cys−NEM, and peak integrals for CH and CH_2 hydrogens obtained under different conditions (PDF)

■ AUTHOR INFORMATION

Corresponding Authors

G. A. Nagana Gowda − *Northwest Metabolomics Research Center, University of Washington, Seattle, Washington 98109, United States; Mitochondria Metabolism Center, Anesthesiology and Pain Medicine, University of Washington, Seattle, Washington 98109, United States;* orcid.org/0000-0002-0544-7464; Email: ngowda@uw.edu

https://doi.org/10.1021/acsomega.2c03482
ACS Omega 2022, 7, 26928−26935

Daniel Raftery − *Northwest Metabolomics Research Center, University of Washington, Seattle, Washington 98109, United States; Mitochondria Metabolism Center, Anesthesiology and Pain Medicine, University of Washington, Seattle, Washington 98109, United States; Fred Hutchinson Cancer Research Center, Seattle, Washington 98109, United States;* orcid.org/0000-0003-2467-8118; Email: draftery@uw.edu

Authors

Vadim Pascua − *Northwest Metabolomics Research Center, University of Washington, Seattle, Washington 98109, United States; Mitochondria Metabolism Center, Anesthesiology and Pain Medicine, University of Washington, Seattle, Washington 98109, United States*

Fausto Carnevale Neto − *Northwest Metabolomics Research Center, University of Washington, Seattle, Washington 98109, United States; Mitochondria Metabolism Center, Anesthesiology and Pain Medicine, University of Washington, Seattle, Washington 98109, United States*

Complete contact information is available at: https://pubs.acs.org/10.1021/acsomega.2c03482

Notes

The authors declare no competing financial interest.

■ ACKNOWLEDGMENTS

The authors gratefully acknowledge financial support from the NIH (R01GM138465, P30DK035816) and a Pilot Grant from the University of Washington Center for Translational Muscle Research (P30AR074990).

■ REFERENCES

(1) Gorin, G.; Martic, P. A.; Doughty, G. Kinetics of the reaction of N-ethylmaleimide with cysteine and some congeners. *Arch. Biochem. Biophys.* **1966**, *115*, 593−597.

(2) Nair, D. P.; Podgórski, M.; Chatani, S.; Gong, T.; Xi, W.; Fenoli, C. R.; Bowman, C. N. The Thiol-Michael Addition Click Reaction: A Powerful and Widely Used Tool in Materials Chemistry. *Chem. Mater.* **2014**, *26*, 724−744.

(3) Northrop, B. H.; Frayne, S. H.; Choudhary, U. Thiol−maleimide "click" chemistry: evaluating the influence of solvent, initiator, and thiol on the reaction mechanism, kinetics, and selectivity. *Polym. Chem.* **2015**, *6*, 3415−3430.

(4) Frayne, S. H.; Murthy, R. R.; Northrop, B. H. Investigation and Demonstration of Catalyst/Initiator-Driven Selectivity in Thiol-Michael Reactions. *J. Org. Chem.* **2017**, *82*, 7946−7956.

(5) Koniev, O.; Wagner, A. Developments and recent advancements in the field of endogenous amino acid selective bond forming reactions for bioconjugation. *Chem. Soc. Rev.* **2015**, *44*, 5495−5551.

(6) Kolb, H. C.; Finn, M. G.; Sharpless, K. B. Click Chemistry: Diverse Chemical Function from a Few Good Reactions. *Angew. Chem. Int. Ed.* **2001**, *40*, 2004−2021.

(7) Friedmann, E.; Marrian, D. H.; Simon-reuss, I. Antimitotic action of maleimide and related substances. *J. Brit. Pharmacol. Chemother.* **1949**, *4*, 105−108.

(8) Horváti, K.; Bõsze, S.; Hudecz, F.; Medzihradszky-Schweiger, H. A simple method for monitoring the cysteine content in synthetic peptides. *J. Pept. Sci.* **2008**, *14*, 838−844.

(9) Kurono, S.; Kaneko, Y.; Niwayama, S. Quantitative protein analysis using $^{13}C_7$-labeled iodoacetanilide and d5-labeled N-ethylmaleimide by nano liquid chromatography/nanoelectrospray ionization ion trap mass spectrometry. *Bioorg. Med. Chem Lett.* **2013**, *23*, 3111−3118.

(10) Nishiyama, J.; Kuninori, T. Assay of thiols and disulfides based on the reversibility of N-ethylmaleimide alkylation of thiols combined with electrolysis. *Anal. Biochem.* **1992**, *200*, 230−234.

(11) Hansen, R. E.; Winther, J. R. An introduction to methods for analyzing thiols and disulfides: Reactions, reagents, and practical considerations. *Anal. Biochem.* **2009**, *394*, 147−158.

(12) Giustarini, D.; Dalle-Donne, I.; Milzani, A.; Fanti, P.; Rossi, R. Analysis of GSH and GSSG after derivatization with N-ethylmaleimide. *Nat. Protoc.* **2013**, *8*, 1660−1669.

(13) Roberts, E.; Rouser, G. Spectrophotometric Assay for Reaction of N-Ethylmaleimide with Sulfhydryl Groups. *Anal. Chem.* **1958**, *30*, 1291−1292.

(14) Tietze, F. Enzymic method for quantitative determination of nanogram amounts of total and oxidized glutathione: applications to mammalian blood and other tissues. *Anal. Biochem.* **1969**, *27*, 502−522.

(15) Brigelius, R.; Muckel, C.; Akerboom, T. P. M.; Sies, H. Identification and quantitation of glutathione in hepatic protein mixed disulfides and its relationship to glutathione disulfide. *Biochem. Pharmacol.* **1983**, *32*, 2529−2534.

(16) Hakuna, L.; Doughan, B.; Escobedo, J. O.; Strongin, R. M. A simple assay for glutathione in whole blood. *Analyst* **2015**, *140*, 3339−3342.

(17) Wang, X.; Chi, D.; Song, D.; Su, G.; Li, L.; Shao, L. Quantification of glutathione in plasma samples by HPLC using 4-fluoro-7-nitrobenzofurazan as a fluorescent labeling reagent. *J. Chromatogr. Sci.* **2012**, *50*, 119−122.

(18) Nolin, T. D.; McMenamin, M. E.; Himmelfarb, J. Simultaneous determination of total homocysteine, cysteine, cysteinylglycine, and glutathione in human plasma by high-performance liquid chromatography: application to studies of oxidative stress. *J. Chromatogr., B: Anal. Technol. Biomed. Life Sci.* **2007**, *852*, 554−561.

(19) Iwasaki, Y.; Saito, Y.; Nakano, Y.; Mochizuki, K.; Sakata, O.; Ito, R.; Saito, K.; Nakazawa, H. Chromatographic and mass spectrometric analysis of glutathione in biological samples. *J. Chromatogr. B* **2009**, *877*, 3309−3317.

(20) Santa, T. Recent advances in analysis of glutathione in biological samples by high-performance liquid chromatography: a brief overview. *J. Drug Discov. Therapeut* **2013**, *7*, 172−177.

(21) Bravo-Veyrat, S.; Hopfgartner, G. High-throughput liquid chromatography differential mobility spectrometry mass spectrometry for bioanalysis: determination of reduced and oxidized form of glutathione in human blood. *Anal. Bioanal. Chem.* **2018**, *410*, 7153−7161.

(22) Fahrenholz, T.; Wolle, M. M.; Kingston, H. M. S.; Faber, S.; Kern, J. C., 2nd; Pamuku, M.; Miller, L.; Chatragadda, H.; Kogelnik, A. Molecular speciated isotope dilution mass spectrometric methods for accurate, reproducible and direct quantification of reduced, oxidized and total glutathione in biological samples. *Anal. Chem.* **2015**, *87*, 1232−1240.

(23) Bláhová, L.; Kohoutek, J.; Lebedová, J.; Bláha, L.; Večeřa, Z.; Buchtová, M.; Míšek, I.; Hilscherová, K. Simultaneous determination of reduced and oxidized glutathione in tissues by a novel liquid chromatography-mass spectrometry method: application in an inhalation study of Cd nanoparticles. *Anal. Bioanal. Chem.* **2014**, *406*, 5867−5876.

(24) Moore, T.; Le, A.; Niemi, A.-K.; Kwan, T.; Cusmano-Ozog, K.; Enns, G. M.; Cowan, T. M. A new LC-MS/MS method for the clinical determination of reduced and oxidized glutathione from whole blood. *J. Chromatogr., B: Anal. Technol. Biomed. Life Sci.* **2013**, *929*, 51−55.

(25) Giustarini, D.; Dalle-Donne, I.; Milzani, A.; Rossi, R. Detection of glutathione in whole blood after stabilization with N-ethylmaleimide. *Anal. Biochem.* **2011**, *415*, 81−83.

(26) Nagana Gowda, G. A.; Pascua, V.; Raftery, D. Extending the Scope of ^{1}H NMR-Based Blood Metabolomics for the Analysis of Labile Antioxidants: Reduced and Oxidized Glutathione. *Anal Chem* **2021**, *93*, 14844−14850.

(27) Kuninori, T.; Nishiyama, J. Some properties of diastereomers formed in the reactions of N-ethylmaleimide with biological thiols. *Agric. Biol. Chem.* **1985**, *49*, 2453−2454.
(28) Sun, X.; Berger, R. S.; Heinrich, P.; Marchiq, I.; Pouyssegur, J.; Renner, K.; Oefner, P. J.; Dettmer, K. Optimized Protocol for the In Situ Derivatization of Glutathione with N-Ethylmaleimide in Cultured Cells and the Simultaneous Determination of Glutathione/Glutathione Disulfide Ratio by HPLC-UV-QTOF-MS. *Metabolites* **2020**, *10*, 292.
(29) Paasche, A.; Schiller, M.; Schirmeister, T.; Engels, B. Mechanistic study of the reaction of thiol-containing enzymes with alpha, beta-unsaturated carbonyl substrates by computation and chemoassays. *ChemMedChem* **2010**, *5*, 869−880.

https://doi.org/10.1021/acsomega.2c03482
ACS Omega 2022, 7, 26928−26935